Volume 1 | Number 1 | Jan 2013 | Pages 1–100

Dalton Transactions

An international journal of inorganic chemistry
www.rsc.org/dalton

ROYAL SOCIETY OF CHEMISTRY

This is an *Accepted Manuscript*, which has been through the Royal Society of Chemistry peer review process and has been accepted for publication.

Accepted Manuscripts are published online shortly after acceptance, before technical editing, formatting and proof reading. Using this free service, authors can make their results available to the community, in citable form, before we publish the edited article. We will replace this *Accepted Manuscript* with the edited and formatted *Advance Article* as soon as it is available.

You can find more information about *Accepted Manuscripts* in the **Information for Authors**.

Please note that technical editing may introduce minor changes to the text and/or graphics, which may alter content. The journal's standard **Terms & Conditions** and the **Ethical guidelines** still apply. In no event shall the Royal Society of Chemistry be held responsible for any errors or omissions in this *Accepted Manuscript* or any consequences arising from the use of any information it contains.

Journal Name

ARTICLE

The first scorpionate ligand based on diazaphosphole

Martin Mlateček[a], Libor Dostál[a], Zdeňka Růžičková[a], Jan Honzíček[b], Jana Holubová[a] and Milan Erben[a,*]

The reaction of $PhBCl_2$ with $1H$-1,2,4-λ^3-diazaphosphole in the presence of NEt_3 gives new scorpionate ligand, phenyl-tris(1,2-diazaphospholyl)borate (PhTdap). Coordination behaviour of this ligand toward transition and non-transition metals has been comprehensively studied. In thallium(I) complex, Tl(PhTdap), κ^2–N,N bonding supported with intramolecular η^3–phenyl coordination has been observed in the solid state. The Tl(PhTdap) also shows unusual intermolecular π-interactions between five-membered diazaphosphole rings and thallium atom giving infinite molecular chains in the crystal. In square planar complex [Pd(C,N–$C_6H_4CH_2NMe_2$)(PhTdap)], κ^2–bonded scorpionate has been detected in both solution and in the solid state. For other studied compounds with central metal ion Ti(IV), Mo(II), Mn(I), Fe(II), Ru(II), Co(II), Co(III), Ni(II) and Cd(II), κ^3–N,N,N coordination pattern was observed. Electronic properties of PhTdap and its ligand-field strength were elucidated from UV-Vis spectra of transition-metal species. The CH/P replacement on going from tris(pyrazolyl)borate to ligand PhTdap causes slight increase in electronic density rendered to the central metal atom. The following order of ligand-field strength has been established: $HB(3,5$-$Me_2pz)_3$ < $PhB(pz)_3$ < $HB(1,2,4$-triazolyl) < $HB(pz)_3$ < $PhB(1,2,4$-triazolyl) < PhTdap. The crystal structures of ten metal complexes bearing new ligand are reported. The possibility of PhTdap coordination through phosphorus atom is also briefly discussed.

Introduction

Poly(pyrazolyl)borates, belonging to the large class of polydentate anionic ligands known also as scorpionates were introduced by Swiatoslaw Trofimenko in 1966.[1] Since the time, it has been shown that these compounds are extremely versatile due to easy modification of their properties by the substitution in the pyrazolyl rings or at the boron atom.[2] Modified ligands could contain various functional groups giving new features not available in parent species.[3] Additional donor atoms are usually attached as exocyclic substituents in pyrazole ring but analogues bearing alternative heterocycles are also known. Thus scorpionates based on imidazole,[4] triazole,[5] tetrazole,[6] oxazole[7] and their regioisomers or derivatives are known, see Figure 1. The presence of additional coordinating atoms in these ligands generally leads to the expansion of scorpionate denticity beyond κ^3 to give, in extreme case, either monomolecular complexes with κ^6– coordinated tris[3-(2-pyridyl)-pyrazol-1-yl]borate ligand[8] or supramolecular structures based on poly(imidazolyl)-, poly(triazolyl)- and poly(tetrazolyl)borates.[9] To the best of our knowledge, no attempts to replace triazole in the scorpionate ligand with phosphorus heterocycle were carried out to date, notwithstanding that suitable azaphospholes are accessible.[10,11] Therefore, we set out to study metal complexes with scorpionates based on 1,2,4-diazaphosphole with the view to extend known series of "azolyl" borates. Herein, we report synthesis, characterization and coordinating behaviour of novel tripodal phenyl-tris(1,2,4-diazaphospholyl)borate. As this species contains phosphorus, typical soft donor atom, incorporated in scorpionate skeleton, some unusual binding modes toward transition metals could be expected.
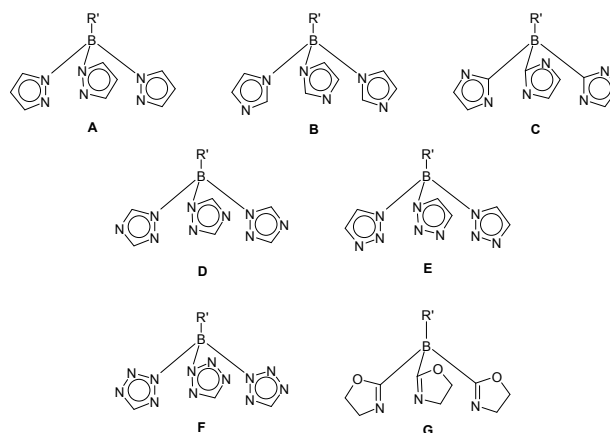

Figure 1. Archetypal borate ligands bearing five-membered heterocyclic rings: A) pyrazol-1-yl, B) imidazol-1-yl, C) imidazol-2-yl, D) 1,2,4-triazol-1-yl E) 1,2,3-triazol-1-yl, F) 1,2,3,4-tetrazol-2-yl and G) oxazol-2-yl.

[a.] Department of General and Inorganic Chemistry, Faculty of Chemical Technology
[b.] Institute of Chemistry and Technology of Macromolecular Materials, Faculty of Chemical Technology, University of Pardubice, Studentská 573, 532 10 Pardubice, Czech Republic.
* Corresponding author. Tel.: +420466037163; fax: +420466037068. E-mail address: milan.erben@upce.cz (M. Erben).
See DOI: 10.1039/x0xx00000x

Results and discussion

Ligand synthesis and the structure of thallium salt

Starting $1H$-1,2,4-λ^3-diazaphosphole (**1**) has been synthesized from 1,3-bis(dimethylamino)-2-phosphaallylchloride and anhydrous hydrazine following methods reported recently.[10, 12] Our attempts to prepare parent hydridoborate ligand by heating of KBH_4 with an excess of **1** were unsuccessful due to decomposition of phosphorus heterocycle giving tarry products bearing P–H bonds. Under milder conditions, **1** reacts with $PhBCl_2$ in the presence of base yielding desired borate anion $[PhB(C_2H_2N_2P)_3]^-$ (PhTdap) which was isolated as thallium(I) salt in moderate yields, see Scheme 1. We note that the use of pure thallium(I) ethoxide is crucial to achieve acceptable yields.

The Tl(PhTdap) (**2**) is air-stable, poorly soluble off-white solid; slow darkening on daylight was observed. The solution ^{1}H and ^{31}P-NMR spectra show that all three heterocycles are equivalent affirming symmetric κ^3–coordination of ligand in the solution.
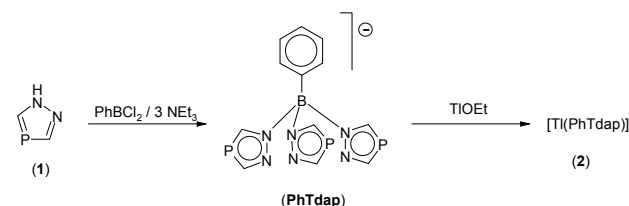
Scheme 1. The preparation of new borate ligand PhTdap.

However, in ^{31}P CP/MAS spectrum two lines were observed at 89 and 91 ppm, respectively, with the intensity ratio 2:1 revealing unsymmetrical coordination pattern in the solid state. It has been further verified by single-crystal X-ray diffraction analysis, see Figure 2. In the crystal structure, the molecule of **2** contains thallium coordinated with two nitrogen atoms (N1 and N1a) in κ^2-*N,N* fashion. Five-membered heterocyclic rings are planar with the deviation from the mean plane not exceeding 0.002(2) Å. The pairs of C–P bonds in each diazapholyl ring differ only slightly confirming delocalization of π-electrons in aromatic system of the heterocycle. Phenyl group shows significant η^3–interaction toward thallium, whereas third diazaphosphole ring remains uncoordinated. This pattern is unprecedented and has not been hitherto described for any known poly(pyrazolyl)borate ligand. Solid **2** also shows unique intermolecular π-interactions between the thallium atom and two aromatic systems of adjacent molecule giving infinite *zig-zag* chains along *a* cell axis, see Scheme 2. Observed thallium-centroid separation of 3.262(1) Å is slightly longer than that (~3.22 Å) reported for $[Tl(\eta^5–P_3C_2Bu^t_2)]$ and related homoleptic hetero-cyclopentadienyl thallium complexes.[13] Polymeric nature of **2** also explains its poor solubility in common organic solvents. The closest observed Tl…Tl distance of 4.5763(4) Å excludes any interactions between thallium atoms in the solid state.
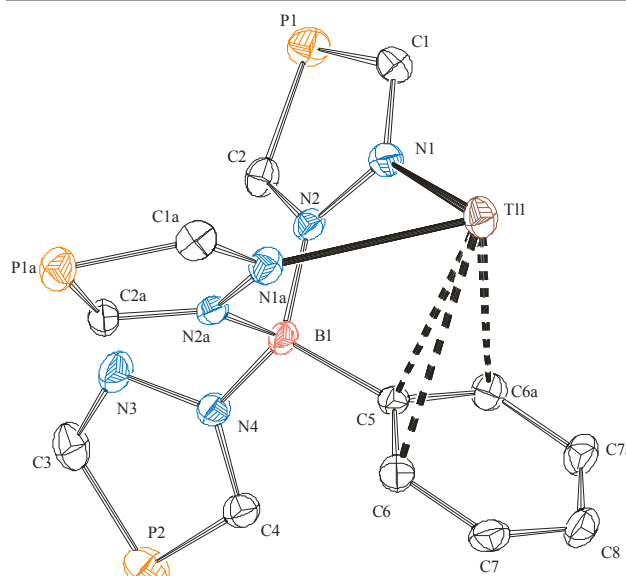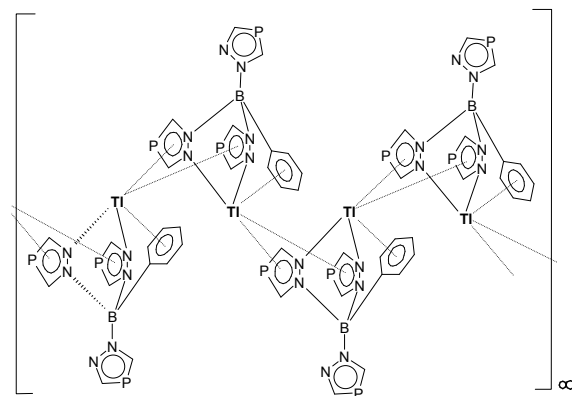

Figure 2. ORTEP drawing of **2** at 50% of probability showing numbering scheme and intramolecular η^3-coordination of phenyl ring. Selected bond distances (Å) and angles (°): Tl1-N1 2.681(3), Tl1-C5 3.063(4), Tl1-C6 3.361(3), and N1-Tl1-N1a 71.27(13).


Scheme 2. Simplified representation of intermolecular π-interactions in crystalline **2**.

Synthesis and characterization of 1:1 complexes

Compound **2** could be easily converted to corresponding alkali metal salts by treatment with aqueous Na_2S, KI or CsI, respectively. These derivatives are slightly water soluble compounds that were not isolated in pure form but characterized only with solution NMR spectroscopy. ^{1}H-NMR spectra consist of two doublets due to equivalent diazaphospholyl rings ($^2J_{PH}$ = 42.3 – 47.7 Hz) accompanied with multiplet of phenyl ring. In ^{31}P-NMR single resonance at 80.5 ± 0.1 ppm is present confirming symmetrical arrangement of PhTdap in the solution. As chemical shifts for Na(Tdap), K(Tdap) and Cs(Tdap), are almost identical, we do not suppose direct interactions between alkali metal ion and PhTdap in D_2O solution. No change in NMR spectra of these solutions has been observed even after a couple of weeks proving the stability of PhTdap toward hydrolysis. Electronic spectra in UV-Vis region showed two intense bands at 255 and 233 nm (ε =

25000–32000 $M^{-1}.cm^{-1}$) attributable to $\pi-\pi^*$ transitions in the aromatic system of the ligand.
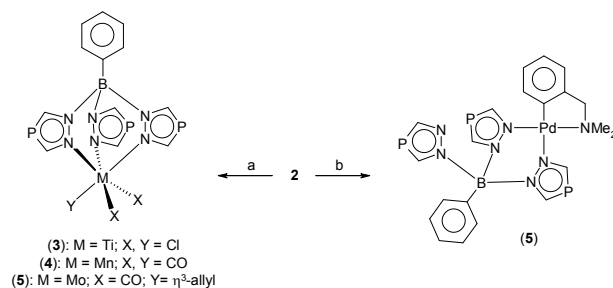
Scheme 3. Syntheses of 1:1 complexes. a) $TiCl_4$, $[Mo(\eta^3-C_3H_5)(MeCN)_2(CO)_2Cl]$ or $[MnBr(CO)_5]$, b) $[PdCl(C,N-C_6H_4CH_2NMe_2)]_2$.

Thallium salt **2** serves as versatile source of PhTdap for syntheses of various metal complexes of the 1:1 stoichiometry, see Scheme 3. Crystalline $[TiCl_3(PhTdap)]$ (**3**) is dark red, air stable solid but it slowly hydrolyses in wet polar solvents. Solution ^1H and ^{13}C-NMR spectra of **3** show only one set of appropriate signals accompanied with single ^{31}P-NMR resonance indicating that PhTdap is symmetrically bonded. The κ^3-N,N,N pattern of ligand in **3** is retained also in the solid state as was confirmed by XRD analysis. Figure 3 shows molecule of **3** where the titanium is pseudooctahedrally coordinated with three nitrogen atoms of PhTdap and three chlorine atoms.
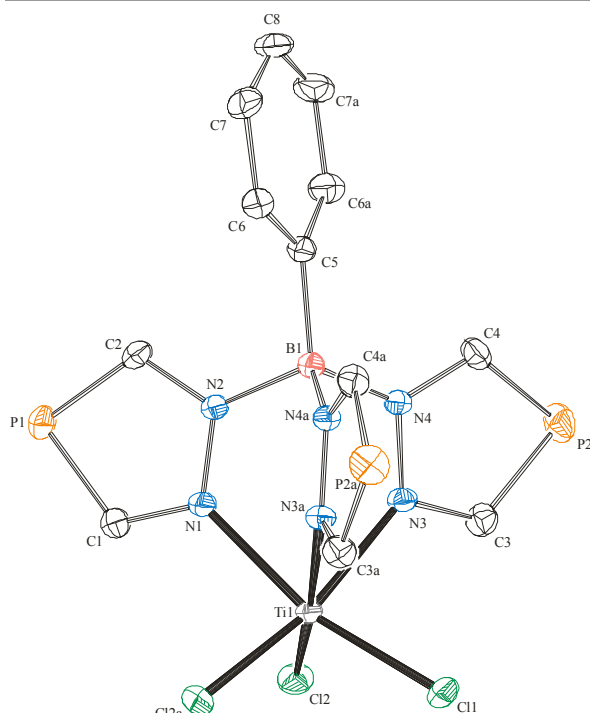

Figure 3. ORTEP drawing of **3** at 50% of probability showing numbering scheme, hydrogen atoms are omitted for clarity. Selected bond distances (Å) and angles (°): Ti1-Cl1 2.2548(6), Ti1-Cl2 2.2294(5), Ti1-N1 2.1467(16), Ti1-N3 2.1761(11), Cl1-Ti1-Cl2 98.46(2), Cl2-Ti1-Cl2a 98.97(2), N1-Ti1-N3 79.78(4), and N3-Ti1-N3a 80.93(4). The effective cone angle: 212°.
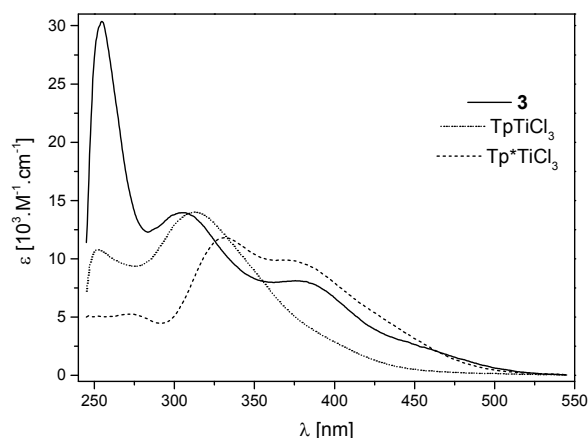

Figure 4. Electronic absorption spectra of **3** and related hydrido-tris(pyrazolyl)borate complexes in THF.

The Ti–N and Ti–Cl bond distances are comparable to those reported for Tp^*TiCl_3 [Tp^* is $HB(3,5-Me_2pz)_3$] and related trichloride complexes.[14] The effective cone angle of 212° resembles the values reported for similar tris(pyrazolyl)borate titanium(IV) compounds. We must note that this is the first crystallographically characterized titanium(IV) trichloride complex bearing scorpionate based on unsubstituted heterocycle. All previously described structures contain substituent in the 3-position of pyrazole ring and thus steric impact of the CH/P exchange could not be simply evaluated. For the purpose of estimation of electronic properties of PhTdap, the UV-Vis spectra of **3** were recorded and compared with related pyrazolyl compounds $TpTiCl_3$ (Tp is $HBpz_3$) and Tp^*TiCl_3, see Figure 4. Since titanium(IV) complexes are formally d^0 systems, the lowest energy absorption bands observed in their electronic spectra are due to charge transfer (CT) transitions. Bright yellow $TpTiCl_3$ has discrete shoulder at ~415 nm followed with distinct maxima at 315 nm. Orange Tp^*TiCl_3 shows absorption shoulder at ~440 nm overlapped with more intense bands at 329 and 367 nm. Dark red **3** absorbs at 468 (shoulder), 376 and 306 nm. Very intense band at 256 nm was unambiguously assigned to $\pi-\pi^*$ transitions in aromatic system of PhTdap (*cf.* data for alkali metal salts and **2**). It has been described previously that in titanium(IV) complexes of the $Tp'TiX_3$ and $Cp'TiX_3$ type (X is halide, Tp' and Cp' is κ^3–tris(pyrazolyl) and η^5–cyclopentadienyl, respectively) the increasing in electron density at the ligand causes the red shift of CT bands.[15] On inspection of obtained data, we can consider that PhTdap is slightly electron richer than Tp congener in this type of complexes.

Manganese(I) complex $[Mn(CO)_3(PhTdap)]$ (**4**) is air-stable light yellow solid but its solutions slowly decomposes on exposure to daylight. One set of signals of diazaphospholyl ring observed in ^1H and ^{13}C NMR spectra together with single resonance ^{31}P indicate κ^3–bonding mode of PhTdap. Infrared spectrum of **4** measured in CCl_4 shows two carbonyl stretching bands at 1943 and 2040 cm^{-1}, the former being broadened. In the solid
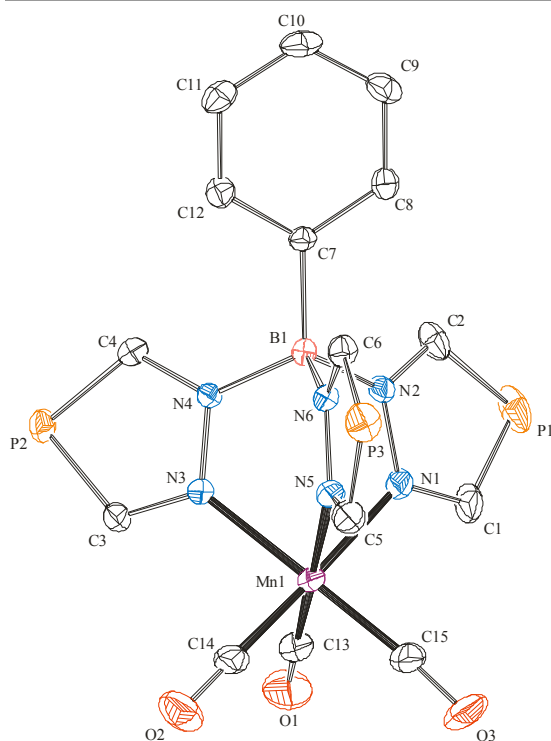
Figure 5. Molecular structure of **4** at 50% of probability showing numbering scheme, hydrogen atoms are omitted for clarity. Selected bond distances (Å) and angles (°): Mn1-N1 2.061(2), Mn1-N3 2.055(2), Mn-N5 2.032(2), Mn1-C13 1.811(3), Mn1-C14 1.811(3), Mn1-C15 1.802(4), N1-Mn1-N3 87.52(10), N1-Mn1-N5 84.30(8), and N3-Mn1-N5 86.02(10). The effective cone angle: 218°.
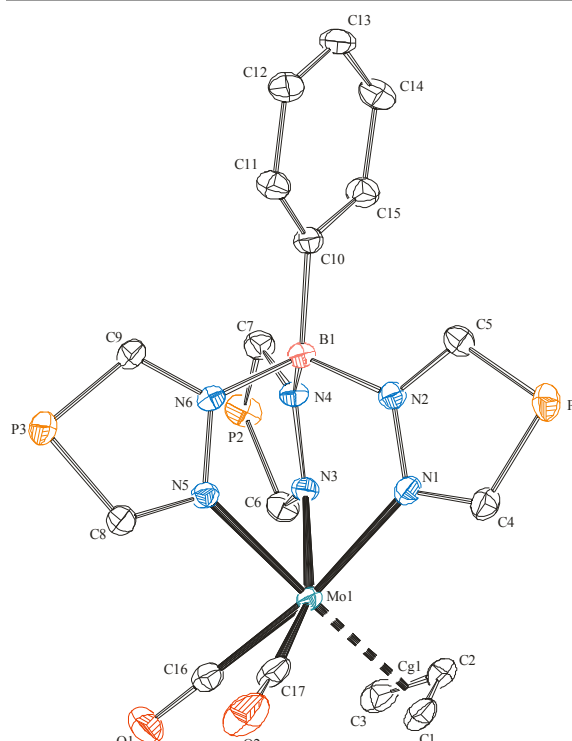
Figure 6. ORTEP drawing of **5** at 50% of probability showing numbering scheme, hydrogen atoms are omitted for clarity. Selected bond distances (Å) and angles (°): Mo1-N1 2.257(2), Mo1-N3 2.288(2), Mo1-N5 2.221(2), Mo1-C16 1.950(2), Mo1-C17 1.942(2), Mo1–Cg1 2.069(1), C16-Mo1-C17 79.16(16), N1-Mo1-N3 82.49(6), N3-Mo1-N5 79.50(6), and N1-Mo1-N5 79.44(6). The effective cone angle: 206°.

state, the absorption at 1943 cm^{-1} is splitted (by 9 cm^{-1}) into two bands. It is typical pattern for piano-stool geometry of Mn(CO)$_3$ fragment. For related complexes TpMn(CO)$_3$, Tp*Mn(CO)$_3$ and pzTpMn(CO)$_3$ (pzTp is Bpz$_4$) were reported ν_{CO} values of 1941/2042, 1927/2032 and 1936/2039 cm^{-1}, respectively.[16] In the case of **4**, electronic properties of PhTdap fall between those of Tp and boron-substituted pzTp ligand.Thus, the CH/P substitution does not markedly increase electron density at the manganese atom. The structure of **4** determined in the solid state is shown in Figure 5. As expected, central metal atom is pseudooctahedrally coordinated with approximate C_{3v} symmetry with manganese and boron located at C_3 axis. Intramolecular bond distances and angles are very close to data reported for abovementioned manganese(I) compounds proving sterical and electronic similarity of PhTdap with Tp, Tp* and pzTp congeners.[17]

In yellow molybdenum(II) complex [Mo(η^3–All)(CO)$_2$(PhTdap)], **5**, diazaphosphole rings of the ligand are not equivalent and two distinct sets of NMR signals (in 2:1 ratio) have been observed approving C_s symmetry of coordinated PhTdap. Similarly, two ^{31}P resonances with 2:1 ratio were found at 81.3 and 83.3 ppm, respectively.

The IR spectrum of **5** shows two characteristic carbonyl stretching absorptions at 1843 and 1932 cm^{-1} (Raman: 1844 and 1930 cm^{-1}) that could be compared with IR data for [Mo(η^3–All)(CO)$_2$Tp], [Mo(η^3–All)(CO)$_2$(pzTp)] and [Mo(η^3–All)(CO)$_2$Tp*] (1874/1958, 1875/1958 and 1832/1925 cm^{-1}, respectively).[18, 19] As the ν_{CO} energy reflects electron density at the molybdenum, electronic properties of PhTdap in **5** could be estimated. Herein, similarly as in the case of titanium(IV) complex, one see that the introduction of phosphorus atom into pyrazolyl ring slightly increases electron density rendered by scorpionate to central metal atom. In the solid state, κ^3–coordination pattern of PhTdap is also present, see Figure 6. Considering the allyl ligand as a single substituent, the **5** possesses distorted octahedral geometry around the molybdenum atom. The allyl fragment adopts an *exo* conformation with respect to Mo(CO)$_2$ unit, in which terminal carbon atoms C1 and C3 eclipse carbonyl carbons C17 and C16, respectively. The bond distance Mo1-N5 was found to be considerably shorter [2.221(2) Å] than those between molybdenum and remaining nitrogen donor atoms [2.257(2), 2.288(2) Å]. This distortion is caused by *trans*-effect of the carbonyl ligands[20] as was previously demonstrated in the series of pseudooctahedral molybdenum(II) complexes.[21] Intramolecular bonds distances and angles are equal within the experimental errors to data reported for corresponding complexes with Tp or Tp* ligand.[19]
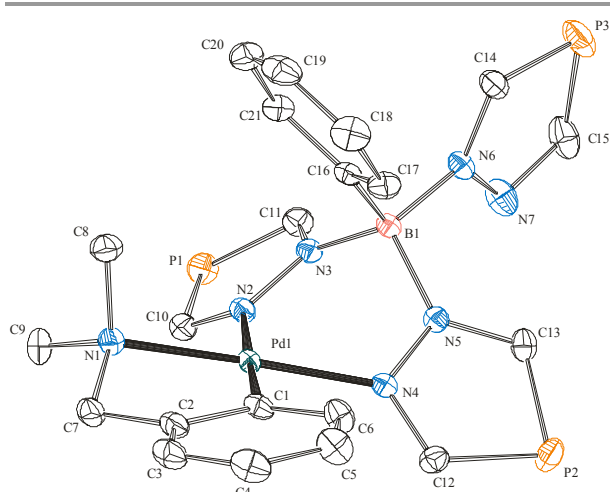
Figure 7. The ORTEP plot of **6** at 50% of probability showing numbering scheme, hydrogen atoms are omitted for clarity. Selected bond distances (Å) and angles (°): Pd1-N1 2.102(2), Pd1-N2 2.152(2), Pd1-N4 2.030(2), Pd1-C1 1.992(2), N1-Pd1-N2 100.08(7), N2-Pd1-N4 85.19(7), N4-Pd1-C1 93.42(8) and N1-Pd1-C1 81.31(8).

From previous examples of 1:1 complexes, it is evident that PhTdap prefers κ^3–bonding pattern, typical for known tris(pyrazolyl)borates. With the view to enforce different coordination mode, we have prepared and characterized palladium(II) complex [Pd(C,N–$C_6H_4CH_2NMe_2$)(PhTdap)], **6**, bearing both PhTdap and C,N-chelated N,N-dimethylbenzylamine (*dmba*) ligand. In the solution, the **6** is stereochemically rigid at ambient temperature. Three inequivalent diazaphospholyl rings present in molecule give six ^{1}H-NMR doublets ($^2J_{PH}$ = 41.9 – 47.9 Hz) that is in line of expected C_1 symmetry. The CH_2 protons of *dmba* appear as AX patterns ($^2J_{HH}$ = 13.3 Hz) along with two singlets of N(CH$_3$)$_2$ protons. Thus we expect ligand PhTdap in this complex behaving as κ^2-chelator. In electronic UV-Vis spectrum are dominating bands of aromatic π-π^* transitions of ligand (257 and 236 nm) accompanied with absorption at 312 nm attributable to CT transition. The X-ray crystal structure of **6**, shown in Figure 7, affirmed square coordination environment at the palladium atom. Central metal and atoms C1, N1, N2 and N4 are almost planar with the deviation from the mean plane not exceeding 0.013(1) Å. The variations in valence angles around the palladium atom (81.31 – 100.08°) are due to different steric requirement of five- and six-membered chelate ring present in the molecule but the sum of these angles is equal to 360.0(3)°. The Pd1–N2 bond distance is significantly elongated by 0.122 Å when compared with Pd1–N4 due to *trans*-influence of aryl *dmba* ligand. The plane of *dmba* aromatic ring and metal plane are not coplanar resulting in dihedral angle C6–C1–Pd1–N4 of 19.5(2)°. Intramolecular bonds and angles correspond to data reported for similar naphtyl derivative [Pd(C,N–$C_{10}H_6CH_2NMe_2$)Tp].[22] In the structure of **6**, no intra- or intermolecular interactions involving aromatic π-systems or phosphorus atoms were observed. Contrary to the structure of **2**, complex **6** shows differences in internal C–P and C–N bonds of diazaphospholyl

rings. The mean distances of C–P and C–N bonds in coordinated heterocycles are of 1.735(5) Å and 1.331(5) Å, respectively, approving significant delocalization of electrons in heteroaromatic π-system. However, for pendant diazaphosphole ring, different lengths of bond pairs P3–C14 / P3–C15 [1.714(2) Å / 1.758(3) Å] and C14–N6 / C15–N7 [1.344(3) Å / 1.318(3) Å] were found. Thus in **6**, uncoordinated heterocycle resembles *N*-substituted heterocyclic diene rather than aromatic diazaphospolyl anion.[23]

Synthesis and characterization of 1:2 complexes

Divalent complexes Fe(PhTdap)$_2$ (**7**), Ru(PhTdap)$_2$ (**8**), Co(PhTdap)$_2$ (**9**), Ni(PhTdap)$_2$ (**10**), and Cd(PhTdap)$_2$ (**11**) were prepared by simple metathesis reactions, see Scheme 4. The reaction proceeds smoothly with moderate to high yield and, irrespective of stoichiometric ratio used, only 1:2 compounds were isolated. Compounds **7** and **11** could be also precipitated from aqueous solution of NaTdap by the addition of soluble iron(II) or cadmium(II) salt, respectively. Prepared complexes were crystallized from hot toluene to give analytically pure material that has been characterized by spectroscopic methods and with single-crystal X-ray diffraction analysis. Studied M(PhTdap)$_2$ compounds show only one set ^{1}H and ^{13}C-NMR signals accompanied with single ^{31}P resonance affirming the expected D_{3d} symmetry of the molecule with κ^3–coordinated PhTdap. Compounds **7**, **8** and **11**, along with abovementioned 1:1 complexes, give resonance of ^{31}P in the region 79.7 – 86.8 ppm (*cf.* **1** in CDCl$_3$: 85.8 ppm), whereas **9** and **10** show significant paramagnetic shift to 251.6 and 195.9 ppm, respectively. Diamagnetic trivalent complex [Co(PhTdap)$_2$]BF$_4$ (**12**) with δ (^{31}P) = 110.0 ppm has been prepared by oxidation of respective divalent species **9** with NOBF$_4$. Molecular structures of **7**, **9** - **11** showed that all these complexes are isomorphous having two independent molecules with minor structural differences in the unit cell. Central metal in divalent complexes **7**, **9** - **11** and in trivalent **12** is sandwiched by two tripodal κ^3–bonded PhTdap ligands adopting octahedral coordination geometry. Figure 8 shows generalized molecular structure of these complexes; Table 1 lists selected interatomic distances and angles.

(**7**): M = Fe(II)
(**8**): M = Ru(II)
(**9**): M = Co(II)
(**10**): M = Ni(II)
(**11**): M = Cd(II)
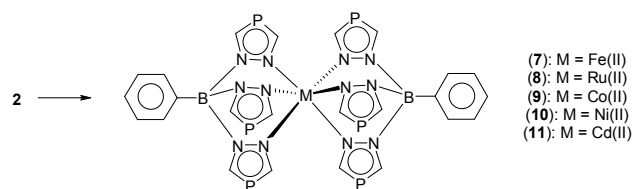
Scheme 4. The preparation of 1:2 complexes. **7**: FeBr$_2$/THF, **8**: Ru(acac)$_3$/Zn/THF, **9**: CoBr$_2$/THF, **10**: [Ni(NH$_3$)$_6$]Cl$_2$/THF, **11**: CdI$_2$/THF
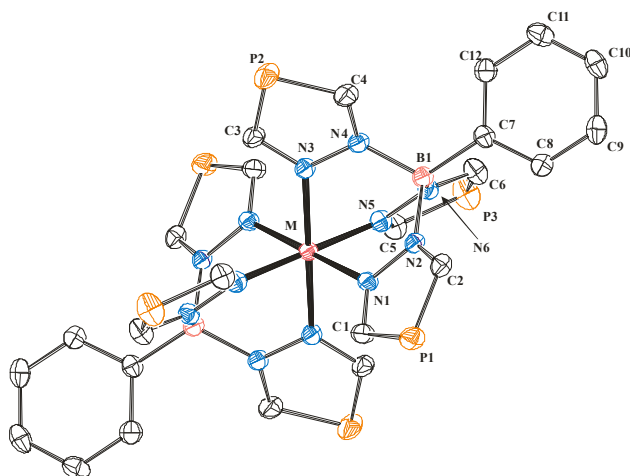
Figure 8. Representative molecular structure of 2:1 complexes of the formula M(PhTdap)$_2$ where M is Fe(II), Co(II), Ni(II), Cd(II) or Co(III). Hydrogen atoms and solvate molecules are omitted for clarity. Atomic positions generated by symmetry operations are not labelled.
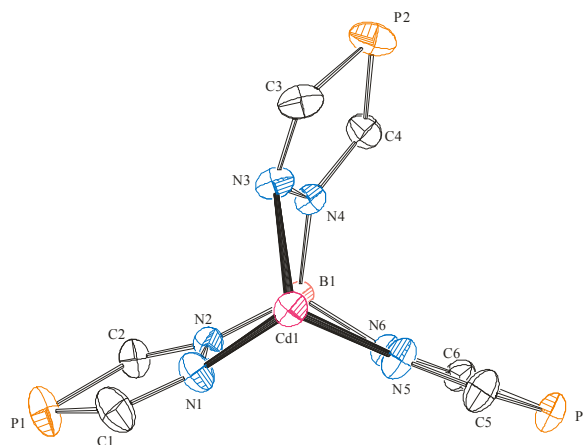

Figure 9. Structural fragment of **11** viewed along the Cd–B axis showing arrangement of diazaphospholyl rings. Hydrogens, phenyl ring and symmetry-generated atoms are omitted for clarity. Selected torsion angles (°): Cd1-N1-N2-B1 20.3(2), Cd1-N1-N2-C2 −159.85(16), Cd1-N3-N4-B1 38.92(12), Cd1-N3-N4-C4 −132.14(13), Cd1-N5-N6-B1 7.0(2), Cd1-N5-N6-C6 174.5(2).

On inspection of these data, it is evident that PhTdap mimics coordination properties of Tp congener toward transition metals and observed geometric parameters are virtually identical to those reported for corresponding MTp$_2$ compounds.[24] Metal ions in **7** and **12** are in almost rigorous octahedral environment with three intraligand N–M–N bond angles near to 90°. This is in agreement with fully low-spin state of these d^6-systems. Octahedral environment in paramagnetic **9** and **10** is slightly deformed as indicated by lowering of N–M–N angle and with higher distortion parameters σ^2_{oct} and λ_{oct}.[25] Elongation of M–N bonds in these two complexes is not only due to larger ionic radii of cobalt(II) and nickel(II) ions but is also the result of antibonding character of partially filled e_{2g}^* orbital in **9** and **10**.

Table 1. Selected interatomic distances (Å), angles (°), parameters of octahedral distortion and ligand cone angle for studied 1:2 complexes.

	7	**9**	**10**	**11**	**12**
Central metal	Fe(II)	Co(II)	Ni(II)	Cd(II)	Co(III)
M–N1	1.980(2)	2.127(4)	2.101(2)	2.345(5)	1.913(5)
M–N3	1.972(2)	2.114(4)	2.079(2)	2.302(4)	1.929(4)
M–N5	1.941(2)	2.082(4)	2.032(2)	2.291(4)	1.932(4)
N1-M-N3	88.81(8)	84.80(16)	87.45(9)	79.91(15)	89.33(19)
N1-M-N5	88.61(8)	86.54(14)	86.29(9)	80.77(15)	89.81(18)
N3-M-N5	88.89(8)	84.89(15)	86.47(10)	84.77(13)	89.97(18)
σ^2_{oct} [deg^2]^a	1.65 1.72^b	23.10 19.65^b	11.97 13.65^b	77.08 71.56^b	0.18
λ_{oct} [1]^a	1.001	1.006	1.004	1.021 1.019^b	1.000
θ [deg]^c	224	215	218	205	227

^{a}Angle variance (σ^2_{oct}) and quadratic elongation (λ_{oct}) of octahedron coordination environment.[25] ^{b}Different values for two crystallographically independent molecules were determined. ^{c}The effective cone angle of PhTdap.[26]

The largest deformation in coordination environment was observed for complex **11**. Two diazaphosphole rings are twisted with the respect to the C_3 axis formed by cadmium and boron atoms yielding partial propeller-like distortion. Third heterocyclic ring is directed toward central metal in almost "ideal" position for maximum overlap of vacant cadmium orbital with sp^2 hybridized nitrogen atom (Figure 9). Similar distortion has been previously reported only for 4-substituted divalent cadmium complex {Cd[HB(4-Br-pz)$_3$]}.[27]

Analysing UV-Vis spectra of octahedral transition-metal species with partially filled d-orbitals, we were able to determine ligand-field strength induced by PhTdap. Table 2 lists the $10Dq$ values for studied compounds having d^6–d^8 electronic configuration; for the purpose of comparison are also included data reported for similar poly(pyrazolyl)borate complexes. Spectroscopic features of **7**, **8** and **12** are typical of low-spin octahedral species. It should be noted that **7** is diamagnetic in the solution at ambient temperature whereas corresponding poly(pyrazolyl)borate derivatives are generally high-spin species or show spin-crossover (SCO) behaviour.[28,29] The SCO process is accompanied with the change in Fe–N bond lengths and in some cases also with decolouring of the complex.[30] The solid **7** does not show any change in IR, Raman or UV-Vis spectra on heating and thus we do not assume SCO up to 180°C. With the view to assess the influence of boron-bonded phenyl group and the presence of heteroatom in PhTdap on spectroscopic properties, we compare spectroscopic data also with iron(II) phenyl-tris(pyrazolyl)borate (PhTp), phenyl-tris(1,2,4-triazolyl)borate (PhTz) and hydrido-tris(1,2,4-triazolyl)borate (Tz) derivatives. Complex Fe(PhTp)$_2$ is diamagnetic[31] in the solution at 295 K with $10Dq$ = 18870 cm^{-1},[32] solid Fe(Tz)$_2$ has $10Dq$ = 19010 cm^{-1},[33] and for Fe(PhTz)$_2$ we have observed 19250 cm^{-1}. From these data the following order of ligand-field strength is evident: Tp$^* <$ PhTp < Tz < Tp < PhTz < PhTdap. Complex **9** is fully paramagnetic at ambient temperature with μ_{eff} value of 4.81 B.M. typical for high-spin

cobalt(II) species and its *10Dq* value is virtually identical to that for pzTp derivative. Oxidation of **9** yields diamagnetic low-spin complex **12** with *10Dq* lower than reported for both pzTp and Tp derivatives. The magnetic and spectroscopic properties of **10** are again close to [Ni(pzTp)$_2$] and are characteristic for nickel(II) octahedral species having electronic spin *S* = 1.

Table 2. The *10Dq* values for metal bis(scorpionate) complexes determined from UV-Vis spectra.

M	*10Dq* (cm^{-1})			
	M(PhTdap)$_2$ [a]	MTp$_2$ [b]	M(pzTp)$_2$ [b]	M(Tp*)$_2$ [b]
Fe(II)	19460	19200 [c]	19100 [c]	12700 [c]
Co(II)	11360	11200 [c]	11400 [c]	10500 [c]
Ni(II)	12090	11900 [c]	12000 [c]	11400 [c]
Ru(II)	25910	– [d]	– [d]	– [d]
Co(III)	22050	21800 [e]	21800 [e]	– [d]

[a] CH$_2$Cl$_2$. [b] From ref. [28] [c] 1,1-dichloroethane. [d] Not reported. [e] CH$_3$CN.

Coordination ability of phosphorus atoms in PhTdap

We have carried out a number of experiments with the view to coordinate PhTdap *via* phosphorus atom. Unfortunately, all attempts led only to the isolation of unreacted starting materials {*e.g* metal carbonyls and their derivatives, CuI.SMe$_2$, AuCl.SMe$_2$, [AuC≡CPh]$_4$, [Rh(COD)Cl]$_2$, [Co(acac)$_2$]$_4$, [Ni(acac)$_2$]$_3$} or to the precipitation of reduced metals. Thus we must state that phosphorus atom in PhTdap does not tend to interact with transition metals. For the inertness of phosphorus is also witnessing the resistance of PhTdap toward hydrogen peroxide or diluted HNO$_3$ when only central metal is oxidized (if possible). In the reaction of M(PhTdap)$_2$ complexes with Ni(COD)$_2$ the precipitate immediately formed at lowered temperatures, but it rapidly decomposes to give nickel metal and starting M(PhTdap)$_2$. In the case of **6,** bearing pendant diazaphosphole ring, entirely insoluble yellow adduct, thermally stable up to 80°C, was isolated from the reaction. In ^{31}P CP/MAS spectrum of **6** two resonances are present at 91.4 (broadened) and 80.1 ppm with integral intensity 2 and 1, respectively. Abovementioned adduct shows two lines as well, but at 85.1 ppm (broadened, 2P) and 0.9 ppm (1P). Significant upfield shift ($\Delta\delta$ = −79.2 ppm) suggests that pendant diazapholyl ring of **6** likely participates in bonding to the nickel atom, but the principle of this interaction remains unclear as we were not able to prepare single-crystal suitable for the determination of adduct molecular structure.

Concluding remarks

In this paper we presented the synthesis and coordination chemistry of unprecedented borate ligand PhTdap based on phosphorus heterocycle. The PhTdap resembles the chemistry and coordination properties of well-known pyrazole-based analogues. The preferred bonding mode toward transition and non-transition metals is highly symmetrical κ^3–*N,N,N* coordination but in some cases κ^2–*N,N* pattern was also observed. For thallium(I) salt, unique κ^2–*N,N*:η^3–Ph coordination accompanied with extensive intermolecular π-

interactions has been found in the solid state. Electronic properties of PhTdap are similar to that of Tp or pzTp derivatives. The phosphorus atoms in the ligand are extraordinary inert and do not tend to coordinate transition metals.

Experimental

Materials

Tris(trimethylsilyl)phosphine and **1** have been prepared following published methods.[34] Complex Fe(PhTz)$_2$ was isolated from reaction of NaPhTz with ammonium iron(II) sulfate in aqueous solution and purified by crystallization from dichloromethane.[35] All preparative reactions and manipulations were carried out under inert atmosphere of argon using standard Schlenk technique. Solvents were dried and deoxygenated in PureSolv MD 7 solvent purification system. Metal salts, NOBF$_4$ and Vilsmeier reagent were used as received from Sigma-Aldrich. Neat thallium ethoxide (Sigma-Aldrich) was heated to 120 °C at 600 Pa for 3 hours to remove residual TlOH and EtOH. Precipitated Tl$_2$O was filtered off using PTFE syringe filter and pure TlOEt has been stored under argon at 4°C.

CAUTION! Thallium is very toxic and care should be taken when handling with its derivatives. Tris(trimethylsilyl)phosphine is pyrophoric and reacts violently with water to give flammable toxic gases. Anhydrous hydrazine is extremely reactive with oxidizing agents including air and should always be prepared and used behind a protective screen in fume-hood.

Spectroscopic measurements

The ^{1}H, ^{13}C and ^{31}P NMR spectra were measured at 300K on a Bruker Avance III 500 MHz instrument equipped with Prodigy CryoProbe; the chemical shifts were referenced to external neat (CH$_3$)$_4$Si or H$_3$PO$_4$, respectively. The ^{31}P CP/MAS NMR spectra were recorded at room temperature on a Bruker Ascend 500 spectrometer at a magnetic field 11.746 T (^{31}P resonance frequency of 202 MHz) with a 3.2 mm DVT CP/MAS probe. The spectra were recorded at the spinning speed 15 and 24 kHz. The Fourier transformation was done on the entire magnetization to improve the signal to noise ratio and to avoid any distortion of the baseline. The processing and acquisition parameters were 3.5 μs π/2 pulse duration, 5 sec delay, 56 W power level, 10000 accumulated scans (external reference NH$_4$H$_2$PO$_4$). IR spectra were recorded on a Nicolet 6700 FTIR spectrometer using single-bounce diamond or silicon ATR crystal. Raman spectra were recorded in the range 4000 – 100 cm^{-1} with a Nicolet iS50 equipped with iS50 Raman module (excitation laser 1064 nm). Electronic absorption spectra (200 – 1080 nm) were run on a Black-Comet C-SR-100 concave grating spectrometer equipped with a dip probe having optical pathway 1 and 10 mm, respectively. Elemental CHN analyses were obtained with a Fisions EA 1108 microanalyzer. Solid samples for elemental analyses were initially dried in vacuum (10^{-2} – 10^{-3} Pa) at 50°C for 12 hours to remove residual or co-crystallized solvents. Melting points were determined in argon-

sealed capillaries using a Stuart SMP-3 melting point apparatus and are uncorrected. Magnetic susceptibility of paramagnetic complexes was measured in the solid state at room temperature on Evans susceptibility balance MSB-AUTO.

Corrections due to diamagnetic contribution of PhTdap were taken in the order to obtain magnetic susceptibility and the spin state of central metal ion.

Table 3 Crystallographic data for 1:1 compounds.

Compound	**2**	**3**	**4**	**5**	**6**
Empirical formula	$C_{12}H_{11}BN_6P_3Tl$	$C_{12}H_{11}BCl_3N_6P_3Ti$	$C_{15}H_{11}BMnN_6O_3P_3$	$C_{17}H_{16}BMoN_6O_2P_3$	$C_{21}H_{23}BN_7P_3Pd$
a (Å)	9.1440 (4)	8.2810 (4)	16.9620(9)	8.7379 (7)	9.4040(16)
b (Å)	10.3091 (8)	10.2920 (3)	10.4820(7)	9.9570 (3)	15.931(4)
c (Å)	17.5949 (8)	11.4621 (10)	24.6311(14)	13.2391 (9)	16.528(6)
α (°)	90	90	90	104.609 (4)	90
β (°)	90	102.607 (5)	112.579(5)	96.252 (7)	100.27(2)
γ (°)	90	90	90	107.110 (3)	90
V (Å³)	1658.61 (17)	953.34 (10)	4043.6(4)	1044.19 (12)	2436.5(12)
Z	4	2	8	2	4
MW	547.36	497.24	481.96	536.02	583.58
Space group	$Pnma$	$P2_1/m$	$P2_1/c$	$P\bar{1}$	$P2_1/c$
D_{calc}/g cm⁻³	2.192	1.732	1.583	1.705	1.591
μ (mm⁻¹)	10.032	1.131	0.920	0.886	0.983
Reflections used	11561	9590	29387	22413	38654
Independent (R_{int})[a]	1997 (0.037)	2295 (0.030)	8927 (0.035)	4771 (0.034)	5531 (0.056)
Observed [$I > 2\sigma(I)$]	1771	2101	6447	4429	4734
Parameters refined	118	133	541	271	298
Max/min $\Delta\rho$/eÅ⁻³	0.75 / -0.90	0.33 / -0.32	0.66 / -0.56	0.60 / −0.61	0.58 / -0.96
GOF[b]	1.118	1.081	1.174	1.095	1.142
$R(F)/wR(F^2)$[c]	0.0208 / 0.0464	0.0219 / 0.0572	0.0407 / 0.1062	0.0221 / 0.0565	0.0240 / 0.0641

Table 4 Crystallographic data for 1:2 complexes.

Compound	**7**	**9**	**10**	**11**	**12**
Empirical formula	$C_{24}H_{22}B_2FeN_{12}P_6$, $2C_7H_8$	$C_{24}H_{22}B_2CoN_{12}P_6$, $2C_7H_8$	$C_{24}H_{22}B_2N_{12}NiP_6$, $2C_7H_8$	$C_{24}H_{22}B_2CdN_{12}P_6$, $1.5C_7H_8$	$C_{24}H_{22}B_2CoN_{12}P_6$, C_6H_6, BF_4, $2CHCl_3$
a (Å)	10.9810 (6)	11.1320 (5)	11.0910 (5)	14.0480 (7)	11.2374 (5)
b (Å)	13.5289 (12)	13.749 (1)	13.6971 (10)	14.0970 (3)	17.1902 (3)
c (Å)	15.9001 (10)	15.6951 (14)	15.7350 (9)	14.1551 (12)	24.3814 (6)
α (°)	91.940 (5)	90.726 (6)	90.977 (6)	66.977 (3)	90
β (°)	99.962 (4)	99.272 (4)	99.368 (4)	61.712 (4)	97.463 (5)
γ (°)	111.752 (5)	112.266 (5)	112.091 (5)	61.256 (3)	90
V (Å³)	2148.4 (3)	2186.9 (3)	2177.3 (2)	2115.4 (2)	4669.9 (3)
Z	2	2	2	2	4
MW	926.09	929.17	928.95	936.58	1148.56
Space group	$P\bar{1}$	$P\bar{1}$	$P\bar{1}$	$P\bar{1}$	$C2/c$
D_{calc}/g cm⁻³	1.432	1.411	1.417	1.398	1.634
μ (mm⁻¹)	0.620	0.657	0.711	0.785	0.975
Reflections used	36582	39918	36709	48084	21548
Independent (R_{int})[a]	9655 (0.041)	9824 (0.051)	9891 (0.049)	12693 (0.031)	5342 (0.038)
Observed [$I > 2\sigma(I)$]	7845	8256	7606	10573	4274
Parameters refined	535	535	535	472	292
Max/min $\Delta\rho$/eÅ⁻³	0.50 / -0.52	2.06 / -0.64	0.78 / -0.52	0.54 / -0.50	3.93 / -2.02
GOF[b]	1.135	1.106	1.135	1.104	1.077
$R(F)/wR(F^2)$[c]	0.0398 / 0.0970	0.0673 / 0.1864	0.0474 / 0.1045	0.0302 / 0.0821	0.0866 / 0.2439

[a] $R_{int} = \sum |F_o^2 - F_{o,mean}^2|/\sum F_o^2$. [b] GOF $= [\sum(w(F_o^2 - F_c^2)^2)/(N_{diffrs} - N_{params})]^{1/2}$ for all data. [c] $R(F) = \sum ||F_o| - |F_c||/\sum |F_o|$ for observed data; $wR(F^2) = [\sum(w(F_o^2 - F_c^2)^2)/(\sum w(F_o^2)^2)]^{1/2}$ for all data.

Crystal structure determination

The structure of **4** contains disordered carbonyl group which was split into two positions with occupancy of about 6:4; this disorder has been treated by SHELXL97 software instructions.

In the same structure, thermal ellipsoids of atoms C13 O1 C14 O2 C15 O3 C113 O4 C114 O5 C115 and C15x were improved with standard ISOR instruction implemented in SHELXL97.[36] There are residual electron maxima and small cavities within

the unit cell originated from the disordered atoms of toluene solvent in structures of **9**, **10**, **11** and **12**. Disorders were treated with ISOR instruction in SHELXL97 program.[36] In the case of **12** the treatment with ISOR instruction led to higher residual electron density in neighboring areas. PLATON/SQUEZZE software[37] was used to correct the data for the presence of disordered solvent in the structure of **11**. A potential solvent volume of 275 Å^3 was found. 82 electrons per unit cell worth of scattering were located in the void. The calculated stoichiometry of solvent was calculated to be one molecule of toluene per unit cell which results in 50 electrons per unit cell. The X-ray data for all studied single-crystals were obtained at 150 K using Oxford Cryostream low-temperature device on a Nonius KappaCCD diffractometer with Mo Kα radiation (λ = 0.71073 Å), a graphite monochromator, and the ϕ and χ scan mod; relevant crystallographic data are listed in Tables 3 and 4. Data reductions were performed with DENZO-SMN. [38] The absorption was neglected. Structures were solved by direct methods (Sir92) [39] and refined by full matrix least-square based on F^2 (SHELXL97). [36] Hydrogen atoms were mostly localized on a difference Fourier map, however to ensure uniformity of treatment of crystal, all hydrogen were recalculated into idealized positions (riding model) and assigned temperature factors $H_{iso}(H)$ = 1.2 U_{eq} (pivot atom) or of 1.5U_{eq} (methyl). H atoms in methyl, methylene moiety and hydrogen atoms in delocalized systems were placed with C–H distances of 0.96, 0.97 and 0.93 Å, respectively. The effective cone angle of PhTdap in studied compound was calculated in accordance with published method[26] using OLEX2 software.[40] Crystallographic data for structural analysis have been deposited with the Cambridge Crystallographic Data Centre, CCDC Nos. CCDC 1406792-1406799, 1416914 and 1416915 for **5**, **7**, **11**, **9**, **10**, **12**, **2**, **3**, **4** and **6**, respectively. Copies of this information may be obtained free of charge from the Director, CCDC, 12 Union Road, Cambridge CB2 1EY, UK (fax: +441223336033 e-mail: deposit@ccdc.cam.ac.uk or www: http://www.ccdc.cam.ac.uk.

Tl(PhTdap) (2)

1300 mg (15.1 mmol) of **1** was dissolved in 75 ml of toluene and 654 µl (800 mg, 5 mmol) of PhBCl$_2$ have been added at 0°C. After stirring for 1 h, 1.5 ml (1090 mg, 10.8 mmol) of NEt$_3$ was added and stirring continued at RT for 12 h. Precipitated [HNEt$_3$]Cl was filtered, washed with 2x10 ml of toluene and to clear filtrate 355 µl (1250 mg, 5 mmol) of TlOEt has been added at once. After stirring for additional 12 h, tan precipitate was filtered, washed with Et$_2$O, pentane and dried in vacuum. Crude product was extracted with boiling acetone on the frit for 3 days, extract was cooled to -20°C giving off-white **2** (2010 mg, yield 72 %). Single-crystals of **2** have been prepared by slow cooling of saturated acetone solution. Mp. 242-243 °C. ^{1}H NMR (acetone-d$_6$): δ 6.74 (m, Ph, 2H), 7.38 (m, Ph, 3H), 8.60 (dd, 3H, $^2J_{PH}$ = 44.6 Hz, $^4J_{HH}$ = 0.8 Hz), 8.90 (dd, 3H, $^2J_{PH}$ = 48.0 Hz, $^4J_{HH}$ = 0.9 Hz). ^{13}C NMR: δ 129.4, 134.8, 164.8 (d, $^1J_{PC}$ = 61.7 Hz), 164.9 (d, $^1J_{PC}$ = 53.3 Hz), C_{ipso} not observed ^{31}P{^{1}H} NMR: δ 79.7. UV-Vis (CH$_2$Cl$_2$, λ_{max}, nm): 255 < 238 nm. Anal. calc. for

C$_{12}$H$_{11}$BN$_6$P$_3$Tl: C, 26.33; H, 2.03; N, 15.35. Found: C, 26.38; H, 2.10; N, 15.26%.

Na(PhTdap)

To stirred suspension of **2** (250 mg, 0.46 mmol) in 5 ml of D$_2$O solid Na$_2$S·9H$_2$O (53 mg, 0.22 mmol) was added and stirring continued for 30 minutes. Black Tl$_2$S and excessive **2** was filtered using PTFE syringe filter and colourless filtrate of NaPhTdap has been spectroscopically characterized. ^{1}H-NMR (D$_2$O): δ 7.04 (m, Ph, 2H), 7.26 (m, Ph, 3H), 8.40 (d, 3H, $^2J_{PH}$ = 42.3 Hz), 8.77 (d, 3H, $^2J_{PH}$ = 47.7 Hz). ^{13}C NMR: δ 127.3, 127.4, 133.2, 162.7 (d, $^1J_{PC}$ = 52.3 Hz), 164.4 (d, $^1J_{PC}$ = 60.9 Hz), C_{ipso} not observed. ^{31}P{^{1}H} NMR (D$_2$O): δ 80.3. UV-Vis (H$_2$O/D$_2$O, λ_{max}, nm): 255 < 232 nm.

K(PhTdap)

Following procedure described for NaPhTdap, colourless solution of KPhTdap was prepared from 300 mg (0.55 mmol) of **2** and 90 mg (0.54 mmol) KI in D$_2$O. ^{1}H-NMR (D$_2$O): δ 7.09 (m, Ph, 2H), 7.33 (m, Ph, 3H), 8.53 (d, 3H, $^2J_{PH}$ = 43.3 Hz), 8.84 (d, 3H, $^2J_{PH}$ = 47.1 Hz). ^{13}C NMR: δ 127.4, 127.5, 133.3, 162.9 (d, $^1J_{PC}$ = 53.2 Hz), 164.5 (d, $^1J_{PC}$ = 60.0 Hz), C_{ipso} not observed. ^{31}P{^{1}H} NMR (D$_2$O): δ 80.4. UV-Vis (H$_2$O/D$_2$O, λ_{max}, nm): 255 < 233 nm.

Cs(PhTdap)

The solution of CsPhTdap was prepared from 250 mg (0.46 mmol) **2** and CsI (110 mg, 0.42 mmol) in 10 ml D$_2$O. ^{1}H-NMR (D$_2$O): δ 7.04 (m, Ph, 2H), 7.26 (m, Ph, 3H), 8.47 (d, 3H, $^2J_{PH}$ = 43.3 Hz), 8.78 (d, 3H, $^2J_{PH}$ = 46.4 Hz). ^{13}C NMR: not measured due to poor solubility. ^{31}P{^{1}H} NMR (D$_2$O): δ 80.5 ppm. UV-Vis (H$_2$O/D$_2$O, λ_{max}, nm): 256 < 233 nm.

[TiCl$_3$(PhTdap)] (3)

1500 mg (2.74 mmol) **2** was suspended in 75 ml of dichloromethane and 300 µl (519 mg, 2.74 mmol) of TiCl$_4$ was added dropwise with stirring continued for 2 h under reflux. Solvent was removed in vacuum and brown residue was extracted with toluene at 50 °C, charcoal has been added and the mixture was filtered. To resulting red filtrate pentane has been added and cooled to -20 °C. After few days, deep red blocks of **3** crystallized (979 mg, yield 72 %). Mp. 140-142 °C (dec.). ^{1}H NMR (CDCl$_3$): δ 7.69 (m, Ph, 3H), 7.96 (m, Ph, 2H), 8.85 (dd, 3H, $^2J_{PH}$ = 40.4 Hz, $^4J_{HH}$ = 0.8 Hz), 9.65 (dd, 3H, $^2J_{PH}$ = 42.4 Hz, $^4J_{HH}$ = 0.8 Hz). ^{13}C NMR (CDCl$_3$): δ 129.2 (Ph), 130.0 (Ph), 134.9 (Ph), 163.6 (d, $^1J_{PC}$ = 57.8 Hz), 173.6 (d, $^1J_{PC}$ = 56.0 Hz), C_{ipso} not observed. ^{31}P{^{1}H} NMR (CDCl$_3$): δ 79.9. UV-Vis [THF, λ_{max}, nm, ε, log(M^{-1}.cm^{-1})]: 468sh (3.45), 376 (3.91), 306 (4.15), 256 (4.33). Anal. calc. for C$_{12}$H$_{11}$BCl$_3$N$_6$P$_3$Ti: C, 28.99; H, 2.23; N, 16.90. Found: C, 28.72; H, 2.29; N, 16.71%.

[Mn(CO)$_3$(PhTdap)] (4)

400 mg (0.73 mmol) **2** and 231 mg (0.73 mmol) of Mn(CO)$_5$Br were stirred in 30 ml of THF for 12h under reflux. After solvent removal, product was extracted with boiling hexane, charcoal was added and filtered. Volume of the filtrate was reduced to minimum and cooled to -20°C. Yellow crystals were filtered off

to give 368 mg (yield 90%) of **4**. Single-crystals of **4** were grown from hot hexane solution on slow cooling to -20°C. Mp.140-141°C. ^{1}H NMR (CDCl$_3$): δ 7.61 (m, Ph, 3H), 7.93 (m, Ph, 2H), 8.80 (d, 3H, $^2J_{PH}$ = 40.9 Hz), 9.17 (d, 3H, $^2J_{PH}$ = 43.0 Hz). ^{13}C NMR (CDCl$_3$): δ 129.0 (Ph), 129.6 (Ph), 135.4 (Ph), 165.9 (d, $^1J_{PC}$ = 58.0 Hz), C_{ipso} not observed, 171.8 (d, $^1J_{PC}$ = 62.2 Hz), 220.5 (CO). ^{31}P{^{1}H} NMR (CDCl$_3$): δ 86.7. IR (cm^{-1}), solid: 1929vs-br, 1955m-sh, 2035s; CCl$_4$: 1945vs, 2040s. Ra (cm^{-1}): 1920vs, 1954vs, 2035s. UV-Vis [CH$_2$Cl$_2$, λ$_{max}$, nm, ε, log(M^{-1}.cm^{-1})]: 347 (3.46), 261sh (4.16), 234 (4.47). Anal. calc. for C$_{15}$H$_{11}$BMnN$_6$O$_3$P$_3$: C, 37.38; H, 2.30; N, 17.44. Found: C, 37.45; H, 2.55; N, 17.26%.

[Mo(η^3-C$_3$H$_5$)(CO)$_2$(PhTdap)] (5)

250 mg (0.46 mmol) of **2** was suspended in 50 ml of THF and the solution of [Mo(η^3-C$_3$H$_5$)(CO)$_3$)]Cl (118 mg, 0.46 mmol) in 30 ml of THF have been added. After 12 h of stirring under reflux the solvent was evaporated and yellow-brown solid extracted with hexane using Soxhlet apparatus. Cooling of saturated hexane solution yielded 187 mg (yield 82%) of **5**. Mp. 235°C (dec.). ^{1}H NMR (CDCl$_3$): δ 1.78 (d, anti-CH$_2$, 2H, $^3J_{HH}$ = 9.6 Hz), 3.73 (d, syn-CH$_2$, 2H, $^3J_{HH}$ = 6.4 Hz), 3.98 (tt, CH, 1H, $^3J_{HH}$ = 9.5 Hz, $^3J_{HH}$ = 6.4 Hz) 7.57 (m, Ph, 3H), 7.84 (m, Ph, 2H), 8.65 (d, 2H, $^2J_{PH}$ = 41.2 Hz), 9.06 (d, 1H, $^2J_{PH}$ = 44.6 Hz), 9.17 (d, 2H, $^2J_{PH}$ = 43.2 Hz), 10.00 (d, 1H, $^2J_{PH}$ = 43.2 Hz). ^{13}C NMR: δ 61.0 (CH$_2$, allyl), 76.4 (CH, allyl), 128.9 (Ph), 129.4 (Ph), 135.5 (Ph), 166.4 (d, $^1J_{PC}$ = 58.3 Hz), 167.4 (d, $^1J_{PC}$ = 56.4 Hz), 167.4 (d, $^1J_{PC}$ = 56.4 Hz), 169.9 (d, $^1J_{PC}$ = 61.8 Hz), 176.9 (d, $^1J_{PC}$ = 61.7 Hz), 227.4 (CO) ppm, C_{ipso} not observed. ^{31}P{^{1}H} NMR: δ 81.3 (2P), 83.3 (1P) ppm. IR (cm^{-1}), solid: 1843vs, 1932vs; CCl$_4$: 1870vs, 1955s. Ra (cm^{-1}): 1844vs, 1930m. UV-Vis [CH$_2$Cl$_2$, λ$_{max}$, nm, ε, log(M^{-1}.cm^{-1})]: 384 (3.21), 256sh (4.49), 235 (4.64). Anal. calc. for C$_{17}$H$_{16}$BMoN$_6$O$_2$P$_3$: C, 38.09; H, 3.01; N, 15.68. Found: C, 38.21; H, 3.13; N, 15.55%.

[Pd(C$_6$H$_4$CH$_2$NMe$_2$)(PhTdap)] (6)

500 mg (0.92 mmol) **2** and 254 mg (0.46 mmol) [Pd(C$_6$H$_4$CH$_2$NMe$_2$)]$_2$Cl$_2$ was boiled in 75 ml of acetone for 12 h. Charcoal has been added and the mixture was filtered. After reducing the volume the filtrate was cooled to -20°C yielding 397 mg (79 %) of colourless **6**. Mp. darkens above 146°C. ^{1}H NMR (CDCl$_3$): δ 1.78 [s, N(CH$_3$)$_2$, 3H], 2.72 [s, N(CH$_3$)$_2$, 3H], 3.26 (d, CH$_2$, 1H, $^2J_{HH}$ = 13.4 Hz), 4.38 (d, CH$_2$, 1H, $^2J_{HH}$ = 13.3 Hz), 6.52 (m, 1H, Ph), 6.87–7.38 (m, 8H, Ph), 8.20 (d, 1H, $^2J_{PH}$ = 41.9 Hz), 8.43 (d, 1H, $^2J_{PH}$ = 43.4 Hz), 8.61 (d, 1H, $^2J_{PH}$ = 42.6 Hz), 8.72 (d, 1H, $^2J_{PH}$ = 44.0 Hz), 8.81 (d, 1H, $^2J_{PH}$ = 44.1 Hz), 9.09 (d, 1H, $^2J_{PH}$ = 47.9 Hz) ppm. ^{13}C NMR: δ 51.2 [N(CH$_3$)$_2$], 53.2 [N(CH$_3$)$_2$], 73.9 (CH$_2$), 121.4 (Ph), 124.7 (Ph), 125.0 (Ph), 125.6 (Ph), 128.2 (Ph), 128.5 (Ph), 128.7 (Ph), 132.7 (Ph), 134.9 (Ph), 135.0 (Ph), 146.0 (C$_{ipso}$), 148.5 (C$_{ipso}$), 164.5 (d, $^1J_{PC}$ = 56.6 Hz), 164.8 (d, $^1J_{PC}$ = 59.1 Hz), 165.5 (d, $^1J_{PC}$ = 61.6 Hz), 166.6 (d, $^1J_{PC}$ = 54.1 Hz), 170.6 (d, $^1J_{PC}$ = 62.9 Hz) ppm. ^{31}P{^{1}H} NMR: δ 81.8, 84.4, 86.4 ppm. UV-Vis [CH$_2$Cl$_2$, λ$_{max}$, nm, ε, log(M^{-1}.cm^{-1})]: 312sh (3.05), 257sh (4.47), 236 (4.71). Anal. calc. for C$_{21}$H$_{23}$BN$_7$P$_3$Pd: C, 43.22; H, 3.97; N, 16.80. Found: C, 43.20; H, 4.01; N, 16.72%.

[Fe(PhTdap)$_2$] (7)

593 mg (1.1 mmol) **2** and 119 mg (0.55 mmol) of FeBr$_2$ were stirred in 50 ml of THF for 1 day at RT. Solvent was removed and pale red solid was extracted with 30 ml of boiling toluene. After the addition of charcoal and filtration the red solution was cooled to -20°C. During few days large crystals of **7** were formed (327 mg, yield 83%). Mp. 360°C dec. ^{1}H NMR (CDCl$_3$): 7.76 (m, Ph, 2H), 7.87 (m, Ph, 3H), 8.22 (d, 3H, $^2J_{PH}$ = 48.6 Hz), 9.26 (d, 3H, $^2J_{PH}$ = 43.2). ^{13}C NMR: 129.0 (Ph), 129.5 (Ph), 135.7 (Ph), 166.9 (d, $^1J_{PC}$ = 57.2 Hz), 174.5 (d, $^1J_{PC}$ = 61.4 Hz), C_{ipso} not observed. ^{31}P{^{1}H} NMR (CDCl$_3$): 79.7. UV-Vis [CH$_2$Cl$_2$, λ$_{max}$, nm, ε, log(M^{-1}.cm^{-1})]: 514 (2.17), 358 (3.98), 314 (4.01), 248sh (4.43), 232 (4.50). Anal. calc. for C$_{24}$H$_{22}$B$_2$FeN$_{12}$P$_6$: C, 38.86; H, 2.99; N, 22.66. Found: C, 39.02; H, 3.22; N, 22.49%.

[Ru(PhTdap)$_2$] (8)

Zinc dust (850 mg, 56 mmol) was submitted to 75 ml of THF and few drops of concentrated HCl were added. After 15 min of stirring, Ru(acac)$_3$ (250 mg, 102 mmol) was added at once and the mixture refluxed with stirring for 20 h. The **2** (379 mg, 204 mmol) was introduced to ochre mixture and reflux continued for next 12 h. Solvents were removed in vacuum and residue extracted with boiling toluene, charcoal was added and mixture filtered. Volume of the filtrate was reduced to minimum, pentane added and cooled to −20°C yielding 244 mg of orange crystals (61 %). Mp. 320°C dec. ^{1}H NMR (benzene-d_6): δ 7.02 (m, Ph, 2H), 7.33 (m, Ph, 3H), 7.79 (d, 3H, $^2J_{PH}$ = 44.2 Hz), 8.81 (d, 3H, $^2J_{PH}$ = 42.0 Hz) ppm. ^{13}C NMR: δ 128.9 (Ph), 129.3 (Ph), 135.9 (Ph), 165.6 (d, $^1J_{PC}$ = 58.5 Hz), 167.5 (d, $^1J_{PC}$ = 63.0 Hz) ppm, C_{ipso} not observed. ^{31}P{^{1}H} NMR: δ 83.0 ppm. UV-Vis [CH$_2$Cl$_2$, λ$_{max}$, nm, ε, log(M^{-1}.cm^{-1})]: 386sh (2.02), 355 (2.21), 312 (2.34), 248sh (4.41), 234 (4.53). Anal. calc. for C$_{24}$H$_{22}$B$_2$N$_{12}$P$_6$Ru: C, 36.63; H, 2.82; N, 21.36. Found: C, 36.72; H, 2.99; N, 21.33%.

[Co(PhTdap)$_2$] (9)

Dark yellow **9** has been prepared from **2** (400 mg, 0.73 mmol) and CoBr$_2$ (80 mg, 0.37 mmol) analogously to method described for **7**. Yield 228 mg (84 %). Mp. 289-290 °C. ^{1}H NMR (CD$_2$Cl$_2$): δ 6.75 (m, Ph, 2H), 7.25 (m, Ph, 3H), 8.70 (d, 3H, $^2J_{PH}$ = 43.9 Hz), 8.87 (d, 3H, $^2J_{PH}$ = 46.1 Hz) ppm. ^{31}P{^{1}H} NMR: 251.6 ppm. μ$_{eff}$ = 4.81±0.02 (B. M. at 293 K). UV-Vis [CH$_2$Cl$_2$, λ$_{max}$, nm, ε, log(M^{-1}.cm^{-1})]: 880br (1.07), 527sh (1.25), 455 (1.67), 307sh (3.08), 245 (4.43). Anal. calc. for C$_{24}$H$_{22}$B$_2$CoN$_{12}$P$_6$: C, 38.70; H, 2.98; N, 22.56. Found: C, 38.89; H, 3.12; N, 22.41%.

[Ni(PhTdap)$_2$] (10)

Pink **10** has been prepared from **2** (250 mg, 0.46 mmol) and [Ni(NH$_3$)$_6$]Cl$_2$ (41 mg, 0.23 mmol) in boiling THF (50 ml) analogously to method described for **7**. Yield 128 mg (75 %). Mp. 318-319 °C. ^{1}H NMR (CDCl$_3$): 7.14–6.94 (m-br, 5H), 7.22 (s-br, 3H), 7.38 (s-br, 3H) ppm. ^{31}P{^{1}H} NMR (toluene-d_8): δ 195.9 ppm. μ$_{eff}$ = 3.19±0.02 (B. M. at 293 K) UV-Vis [CH$_2$Cl$_2$, λ$_{max}$, nm, ε, log(M^{-1}.cm^{-1})]: 827 (1.10), 571sh (1.07), 500 (1.20), 250sh (4.01), 239 (4.13). Anal. calc. for C$_{24}$H$_{22}$B$_2$N$_{12}$NiP$_6$: C, 38.71; H, 2.98; N, 22.57. Found: C, 38.82; H, 3.09; N, 22.41%.

[Cd(PhTdap)₂] (11)

Colourless crystals of **11** have been prepared from **2** (350 mg, 0.64 mmol) and CdI₂ (117 mg, 0.32 mmol) analogously to method described for **7**. Yield 196 mg (77 %). Mp. 162-163 °C. ^{1}H NMR (CDCl₃): δ 7.6 (m, Ph, 5H), 8.69 (d, 3H, $^2J_{PH}$ = 43.5 Hz), 8.96 (d, 3H, $^2J_{PH}$ = 42.8 Hz). ^{13}C NMR (CDCl₃): δ 128.9 (Ph), 129.4 (Ph), 135.6 (Ph), 166.2 (d, $^1J_{PC}$ = 57.5 Hz), 167.4 (d, $^1J_{PC}$ = 63.5 Hz), C_{ipso} not observed. ^{31}P{^{1}H} NMR (CDCl₃): δ 83.7. UV-Vis [CH₂Cl₂, λ_{max}, nm, ε, log(M^{-1}.cm^{-1})]: 249sh (4.49), 230 (4.74). Anal. calc. for C₂₄H₂₂B₂CdN₁₂P₆: C, 36.10; H, 2.78; N, 21.05. Found: C, 36.21; H, 2.28; N, 20.89%.

[Co(PhTdap)₂]BF₄ (12)

125 mg (0.17 mmol) of **9** was dissolved in CH₂Cl₂ and to this solution 19.6 mg (0.17 mmol) of NOBF₄ in 15 ml of CH₂Cl₂ was added. Stirred mixture was heated for 20 min when the colour changed from pale orange to dark red and bubbles of NO were ceased. After solvent removal, the crude **12** was dissolved in CHCl₃ and charcoal was added. After filtration and addition of pentane the mixture was cooled to -20°C affording orange crystals (98 mg, yield 71 %). Single-crystals of **12** were grown from chloroform solution overlayered with benzene at RT. Mp. 189-191°C. ^{1}H NMR (CDCl₃): δ 9.40 (d, 6H, $^2J_{PH}$ = 40.1 Hz), 8.2 (m, 3H, Ph), 7.81 (m, 2H, Ph) ppm. ^{13}C NMR: δ 129.9 (Ph), 130.9 (Ph), 135.2 (Ph), 169.0 (d, $^1J_{PC}$ = 63.9 Hz), 175.2 (d, $^1J_{PC}$ = 68.1 Hz) ppm, C_{ipso} not observed. ^{31}P NMR: 110.1 ppm. UV-Vis [CH₂Cl₂, λ_{max}, nm, ε, log(M^{-1}.cm^{-1})]: 475sh (2.21), 353sh (3.39), 256 (4.56), 232 (4.64). Anal. calc. for C₂₄H₂₂B₃CoF₄N₁₂P₆: C, 38.26; H, 2.83; N, 21.42. Found: C, 38.49; H, 2.89; N, 21.30%.

References

1   S. Trofimenko, *J. Am. Chem. Soc.*, 1966, **88**, 1842-1844.
2   C. Pettinari and S. Trofimenko, *Scorpionates Two*, Imperial College Press, 2008; S. Trofimenko, *Scorpionates: The Coordination Chemistry of Polypyrazolylborate Ligands*, Imperial College Press, 1999.
3   A. Otero, J. Fernandez-Baeza, A. Lara-Sanchez and L. F. Sanchez-Barba, *Coord. Chem. Rev.*, 2013, **257**, 1806-1868; S. Trofimenko, *Chem. Rev.*, 1972, **72**, 497-509; S. Trofimenko, *Chem. Rev.*, 1993, **93**, 943-980; J. Reglinski and M. D. Spicer, *Coord. Chem. Rev.*, 2015, **297–298**, 181-207.
4   R. Fränkel, U. Kernbach, M. Bakola-Christianopoulou, U. Plaia, M. Suter, W. Ponikwar, H. Nöth, C. Moinet and W. P. Fehlhammer, *J. Organomet. Chem.*, 2001, **617-618**, 530-545; A. Biffis, G. G. Lobbia, G. Papini, M. Pellei, C. Santini, E. Scattolin and C. Tubaro, *J. Organomet. Chem.*, 2008, **693**, 3760-3766; Effendy, G. Gioia Lobbia, M. Pellei, C. Pettinari, C. Santini, B. W. Skelton and A. H. White, *J. Chem. Soc. Dalton*, 2001, 528-534; C. Janiak, S. Temizdemir and C. Roehr, *Z. Anorg. Allg. Chem.*, 2000, **626**, 1265-1267.
5   B. C. Hughes, Z. Lu and D. M. Jenkins, *Chem. Commun.*, 2014, **50**, 5273-5275;   C. Janiak, T. G. Scharmann, P. Albrecht, F. Marlow and R. Macdonald, *J. Am. Chem. Soc.*, 1996, **118**, 6307-6308; C. Janiak, T. G. Scharmann, H. Hemling, D. Lentz and J. Pickardt, *Chem. Ber.*, 1995, **128**, 235-244; C. Janiak, *J. Chem. Soc., Chem. Commun.*, 1994, 545-548.
6   C. J. Snyder, P. D. Martin, M. J. Heeg and C. H. Winter, *Chem.-Eur. J.*, 2013, **19**, 3306-3310.
7   S. R. Neal, A. Ellern and A. D. Sadow, *J. Organomet. Chem.*, 2011, **696**, 228-234; J. F. Dunne, J. Su, A. Ellern and A. D. Sadow, *Organometallics*, 2008, **27**, 2399-2401.
8   A. J. Amoroso, J. C. Jeffery, P. L. Jones, J. A. McCleverty, L. Rees, A. L. Rheingold, Y. Sun, J. Takats, S. Trofimenko, M. D. Ward and G. P. A. Yap, *J. Chem. Soc., Chem. Commun.*, 1995, 1881-1882; H. Adams, S. R. Batten, G. M. Davies, M. B. Duriska, J. C. Jeffery, P. Jensen, J. Lu, G. R. Motson, S. J. Coles, M. B. Hursthouse and M. D. Ward, *Dalton Trans.*, 2005, 1910-1923.
9   C. Janiak, T. G. Scharmann, P. Albrecht, F. Marlow and R. Macdonald, *J. Am. Chem. Soc.*, 1996, **118**, 6307-6308; C. Wang, T. Zhang and W. Lin, *Chem. Rev.*, 2011, **112**, 1084-1104; M. Pellei, G. G. Lobbia, G. Papini and C. Santini, *Mini-Rev. Org. Chem.*, 2010, **7**, 173-203.
10 A. Schmidpeter and A. Willhalm, *Angew. Chem.*, 1984, **96**, 901-902.
11 W. Rösch, T. Facklam and M. Regitz, *Tetrahedron*, 1987, **43**, 3247-3256.
12 J.-W. Wang, L.-Y. Ding, B.-Q. Wang, Y.-Y. He, Y. Guo, X.-F. Jia and W. Zheng, *J. Mol. Struct.*, 2014, **1058**, 62-70.
13 M. D. Francis, P. B. Hitchcock, J. F. Nixon, H. Schnöckel and J. Steiner, *J. Organomet. Chem.*, 2002, **646**, 191-195.
14 K. Michiue, I. Steele, O. L. Casagrande and R. F. Jordan, *Acta Crystallogr., Sect. E: Struct. Rep. Online*, 2006, **62**, m2297-m2298; A. Antiñolo, F. Carrillo-Hermosilla, A. E. Corrochano, J. Fernández-Baeza, M. Lanfranchi, A. Otero and M. A. Pellinghelli, *J. Organomet. Chem.*, 1999, **577**, 174-180; C. Chen and R. F. Jordan, *J. Organomet. Chem.*, 2010, **695**, 2543-2547; M. P. Gil and O. L. Casagrande Jr, *J. Organomet. Chem.*, 2004, **689**, 286-292.
15 R. Gazzi, F. Perazzolo, S. Sostero, A. Ferrari and O. Traverso, *J. Organomet. Chem.*, 2005, **690**, 2071-2077; A. Hafner and J. Okuda, *Organometallics*, 1993, **12**, 949-950; M. Erben, A. Růžička, M. Picka and I. Pavlík, *Magn. Reson. Chem.*, 2004, **42**, 414-417; J. Pinkas, A. Lycka, P. Sindelar, R. Gyepes, V. Varga, J. Kubista, M. Horacek and K. Mach, *J. Mol. Cat. A: Chem.*, 2006, **257**, 14-25; M. Erben, J. Merna, S. Hermanová, I. Císařová, Z. Padělková and M. Dušek, *Organometallics*, 2007, **26**, 2735-2741.
16 D. M. Tellers, S. J. Skoog, R. G. Bergman, T. B. Gunnoe and W. D. Harman, *Organometallics*, 2000, **19**, 2428-2432.
17 J. H. MacNeil, A. W. Roszak, M. C. Baird, K. F. Preston and A. L. Rheingold, *Organometallics*, 1993, **12**, 4402-4412; J. E. Joachim, C. Apostolidis, B. Kanellakopulos, R. Maier, N. Marques, D. Meyer, J. Müller, A. Pires de Matos, B. Nuber, J. Rebizant and M. L. Ziegler, *J. Organomet. Chem.*, 1993, **448**, 119-129.
18 S. Trofimenko, *J. Am. Chem. Soc.*, 1969, **91**, 588-595.
19 Y. D. Ward, L. A. Villanueva, G. D. Allred, S. C. Payne, M. A. Semones and L. S. Liebeskind, *Organometallics*, 1995, **14**, 4132-4156; D. S. Frohnapfel, P. S. White, J. L. Templeton, H. Rüegger and P. S. Pregosin, *Organometallics*, 1997, **16**, 3737-3750.
20 B. J. Coe and S. J. Glenwright, *Coord. Chem. Rev.*, 2000, **203**, 5-80.
21 J. Honzíček, P. Kratochvíl, J. Vinklárek, A. Eisner and Z. Padělková, *Organometallics*, 2012, **31**, 2193-2202; J. Honzíček, I. Honzíčková, J. Vinklárek and Z. Růžičková, *J. Organomet. Chem.*, 2014, **772–773**, 299-306.
22 J.-M. Valk, F. Maassarani, P. van der Sluis, A. L. Spek, J. Boersma and G. van Koten, *Organometallics*, 1994, **13**, 2320-2329.
23 K. Polborn, A. Schmidpeter, G. Markl and A. Willhalm, *Z.Naturforsch.(B)*, 1999, **54**, 187-192.
24 F. Allen, *Acta Crystallogr., Sect. B: Struct. Sci.*, 2002, **58**, 380-388.

ARTICLE

Journal Name

25 K. Robinson, G. V. Gibbs and P. H. Ribbe, *Science*, 1971, **172**, 567-570.

26 G. G. Lobbia, C. Pettinari, F. Marchetti, B. Bovio and P. Cecchi, *Polyhedron*, 1996, **15**, 881-890.

27 G. G. Lobbia, B. Bovio, C. Santini, P. Cecchi, C. Pettinari and F. Marchetti, *Polyhedron*, 1998, **17**, 17-26; D. L. Reger, S. S. Mason, A. L. Rheingold and R. L. Ostrander, *Inorg. Chem.*, 1993, **32**, 5216-5222.

28 D. C. L. De Alwis and F. A. Schultz, *Inorg. Chem.*, 2003, **42**, 3616-3622.

29 Y. Sohrin, H. Kokusen and M. Matsui, *Inorg. Chem.*, 1995, **34**, 3928-3934.

30 30. P. Hamon, J.-Y. Thépot, M. Le Floch, M.-E. Boulon, O. Cador, S. Golhen, L. Ouahab, L. Fadel, J.-Y. Saillard and J.-R. Hamon, *Angew. Chem., Int. Ed.*, 2008, **47**, 8687-8691; R. A. Binstead and J. K. Beattie, *Inorg. Chem.*, 1986, **25**, 1481-1484.

31 J. P. Jesson, S. Trofimenko and D. R. Eaton, *J. Am. Chem. Soc.*, 1967, **89**, 3158-3164.

32 C. Reus, K. Ruth, S. Tüllmann, M. Bolte, H.-W. Lerner, B. Weber, M. C. Holthausen and M. Wagner, *Eur. J. Inorg. Chem.*, 2011, **2011**, 1709-1718.

33 C. Janiak, *Chem. Ber.*, 1994, **127**, 1379-1385.

34 E. Niecke and H. Westermann, *Synthesis-Stuttgart*, 1988, 330-330; T. E. Cole, R. Quintanilla, B. M. Smith and D. Hurst, *Tetrahedron Lett.*, 1992, **33**, 2761-2764.

35 K.-B. Shiu, J. Y. Lee, W. Yu, C. Ming-Chu, W. Sue-Lein and L. Fen-Ling, *J. Organomet. Chem.*, 1993, **453**, 211-219.

36 G. M. Sheldrick, *SHELXL97*, (2008) SHELXL-97, University of Göttingen, Göttingen.

37 P. van der Sluis and A. L. Spek, *Acta Crystallogr., Sect. A: Found. Crystallogr.*, 1990, **46**, 194-201.

38 Z. Otwinowski and W. Minor, *Methods Enzymol.*, 1997, **276**, 307-326.

39 A. Altomare, G. Cascarano, C. Giacovazzo and A. Guagliardi, *J. Appl. Crystallogr.*, 1993, **26**, 343-350.

40 O. V. Dolomanov, L. J. Bourhis, R. J. Gildea, J. A. K. Howard and H. Puschmann, *J. Appl. Crystallogr.*, 2009, **42**, 339-341.

Dalton Transactions Accepted Manuscript
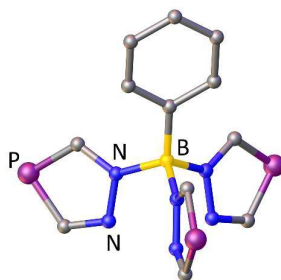
New tripod ligand phenyl-tris(1,2,4-diazaphospholyl)borate has been prepared and its

coordination behaviour toward transition and non-transition metals was studied.